Gut microbiota dysbiosis exacerbates microscopic polyangiitis via toll-like receptor 7

B. Yang, L. Chu, S. Lu, W. Tang, C. Xue

Department of Nephrology, the Second Affiliated Hospital of Guangxi Medical University, Nanning, Guangxi, China.

Abstract

Objective

Anti-neutrophil cytoplasmic antibody-associated vasculitis (AAV) is closely associated with factors such as genetic predisposition, environmental pollution, medications, and infections. Some bacteria have been definitively linked to AAV. Although gut microbiota dysbiosis has been confirmed in individuals with AAV, the specific role of this dysbiosis and the associated mechanisms contributing to AAV pathogenesis remain unexplored. The most common type of AAV in China is microscopic polyangiitis (MPA).

Methods

We used propylthiouracil/phorbol 12-myristate 13-acetate (PMA/PTU) to establish a rat model of MPA. We then administered ceftriaxone sodium to induce dysbiosis of the rat intestinal microflora. We determined differences in gut microbiota using 16sRNA analysis, the degree of kidney and lung injury in rats using haematoxylin-eosin staining, the level of inflammatory factors in peripheral blood using an enzyme-linked immunosorbent assay, the distribution of splenic lymphocyte subpopulations using flow cytometry, the expression of Toll-like receptor 7 (TLR7) in the colon using Western blotting, and the release of neutrophil extracellular traps (NETs) from kidneys using immunofluorescence to assess the impact of gut dysbiosis on MPA.

Results

The results showed that the MPA rat model displayed characteristics consistent with those of human MPA patients. The gut microbiota in rats in the gut dysbiosis group significantly differed from that in rats in the MPA group. Gut microbiota dysbiosis triggered increased release of renal NETs through activation of TLR7 protein, exacerbated microinflammation, increased peripheral blood Interleukin-1β, interleukin-6, C-reactive protein, and tumour necrosis factor-α, disrupted immune homeostasis, and increased the number of CD4+ T cells, CD8+ T cells, and Th17 cells through TLR7 signalling.

Conclusion

Our findings show that microbiota dysbiosis led to increased release of NETs, more severe microinflammation, disruption of immune homeostasis, and exacerbated organ damage in the kidneys of MPA rats through activation of TLR7.

Key words

microscopic polyangiitis, autoimmunity, gut microbiota dysbiosis, neutrophil extracellular traps, rat model, toll-like receptor 7

*Binglan Yang, MD**
*Liepeng Chu, MD**
Shurong Lu, MD
Wenglv Tang, MMed
Chao Xue, Prof.

**Contributed equally.*

Please address correspondence to:
Chao Xue
Department of Nephrology,
The Second Affiliated Hospital of
Guangxi Medical University,
Nanning, Guangxi, 530000, China.
E-mail: xuechao@stu.gxmu.edu.cn

Received on March 16, 2025; accepted in revised form on September 19, 2025.

Funding: this work was supported by the Joint Project on Regional High-Incidence Diseases Research of Guangxi Natural Science Foundation under grant (no. 2024GXNSFAA999092), The Youth Science Foundation of Guangxi Medical University under grant (no. GXMUYSF202522), the Guangxi Health Commission Key Laboratory of Medical Genetics and Genomic (no. GXKMGG202303), Guangxi NaturalScience Foundation Program (no. 2018GXNSFAA281122), the Guangxi Health Commission self-financial project (no. Z-A20230648), the Guangxi Natural Science Foundation (Project title: Research on the Improvement of Renal Injury in ANCA-Associated Vasculitis by Short-Chain Fatty Acids through Promoting Macrophage M2 Polarization, grant no. 2025GXNSFAA069215), Project for Enhancing the Basic Scientific Research Capacity of Young and Middle-aged Teachers in Guangxi Colleges and Universities (Project title: Research on the Role and Mechanism of Short-Chain Fatty Acids inANCA-Associated Vasculitis Based on Multi-Omics Analysis, grant no. AB25069056).

Competing interests: none declared.

Introduction

Anti-neutrophil cytoplasmic antibody-associated vasculitis (AAV) is an autoimmune disease with an unclear aetiology. Research has suggested that AAV is strongly associated with factors such as genetic predisposition, environmental pollution, medication use, and previous infections (1-3). AAV typically manifests as multiple organ dysfunction syndrome (MODS), with the kidneys being the most commonly affected organ. The respiratory system is most affected among the extra-renal manifestations (4). Pulmonary disease is the hallmark feature of the disease and present in 90% of cases (5). Granulomatous inflammation in the lung is the characteristic finding, and vast granulocytic inflammation is non-specific (4). Research has shown that untreated AAV has a mortality rate of approximately 60% at 6 months, which can increase to 80% at 12 months (6). Treatment often includes use of corticosteroids and long-term immunosuppression (7), which entail considerable side effects and may result in disease progression to chronic and recurrent states. The increasing age of China's population is accompanied by a rising incidence of AAV, which is a significant health concern for middle-aged and elderly people (8-10). There are several types of AAV, including granulomatosis with polyangiitis (GPA) (11), microscopic polyangiitis (MPA) (11, 12), and eosinophilic granulomatosis with polyangiitis (EGPA) (13). MPA is the most prevalent in China and predominantly myeloperoxidase (MPO)-positive AAV (MPO-AAV) (15). Although the specific aetiology of AAV remains unclear (14), certain bacteria are known to be associated with the disease. For instance, two bacterial-derived peptides can trigger autoimmune responses against anti-neutrophil cytoplasmic antibody (ANCA) automatic engines and induce glomerulonephritis in mice (7, 15). Additionally, *Staphylococcus aureus* infections have been associated with relapses in granulomatosis with polyangiitis (EGPA) (18). Dysbiosis caused by infections or antibiotic use may trigger an abnormal immune response in genetically susceptible individuals, leading to systemic vasculitis (19). A case-control study on a European population demonstrated an enrichment of *Enterobacteriaceae, Lactobacillaceae*, and *Streptococcaceae* in patients with EGPA, and these bacteria may influence the development of EGPA by elevating the abundance of $CD4^+$ T cells (especially the Th1/Th17 subpopulation) in the intestinal mucosa. However, there has been no report on the mechanism through which gut microbiota dysbiosis is involved in MPA (16).

The aim of the present study was to examine the effects of gut microbiota dysbiosis on MPA rats. To this end, we established an MPA rat model using propylthiouracil/phorbol 12-myristate 13-acetate (PMA/PTU) and induced gut microbiota dysbiosis using ceftriaxone sodium (17). We subsequently assessed kidney and lung damage, renal neutrophil extracellular trap (NET) formation, and changes in T lymphocyte subgroups in the spleen to explore the impact of gut microbiota dysbiosis on MPA progression.

Materials and methods

Animals

Wistar-Kyoto (WKY) rats were purchased from Beijing Vital River Laboratory Animal Technology Co., Ltd., and housed in a specific pathogen-free (SPF) animal facility at Guangxi Medical University under a 12-h light/dark cycle. They were provided with sterile acidified water and irradiated food. The breeding and use of all rats in this study were conducted in accordance with the protocol approved by the Animal Ethics Committee of Guangxi Medical University no: 202209021).

Animal treatment

A total of 30 clean healthy male WKY rats, aged 8–12 weeks and weighing approximately 190–210 g, were used in this study. They were randomly divided into five groups: control group (n=6), MPA model group (MPA group, n=6), intestinal microbiota imbalance group (IM group, n=6), Toll-like receptor 7 (TLR7) agonist group (IM+ R837group, n=6), and TLR7 inhibitor group (IM+ M5049 group, n=6). All

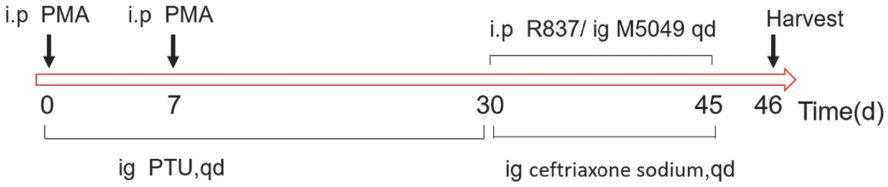

Fig. 1. Study flowchart.

rats were housed in the Experimental Animal Centre of Guangxi Medical University. In the MPA group, the rats were orally administered the antithyroid drug PTU at a dose of 20 mg/kg per day for 30 days and then intraperitoneally injected with 1 μg of PMA on days 0 and 7 to induce NET formation. Vasculitis in all other experimental groups was also induced using the method described above. Additionally, in the IM group, rats were orally administered a solution of ceftriaxone sodium at a concentration of 0.12 g/mL and dose of 0.01 mL/g body weight once daily. In the IM+R837 group, the rats were intraperitoneally injected

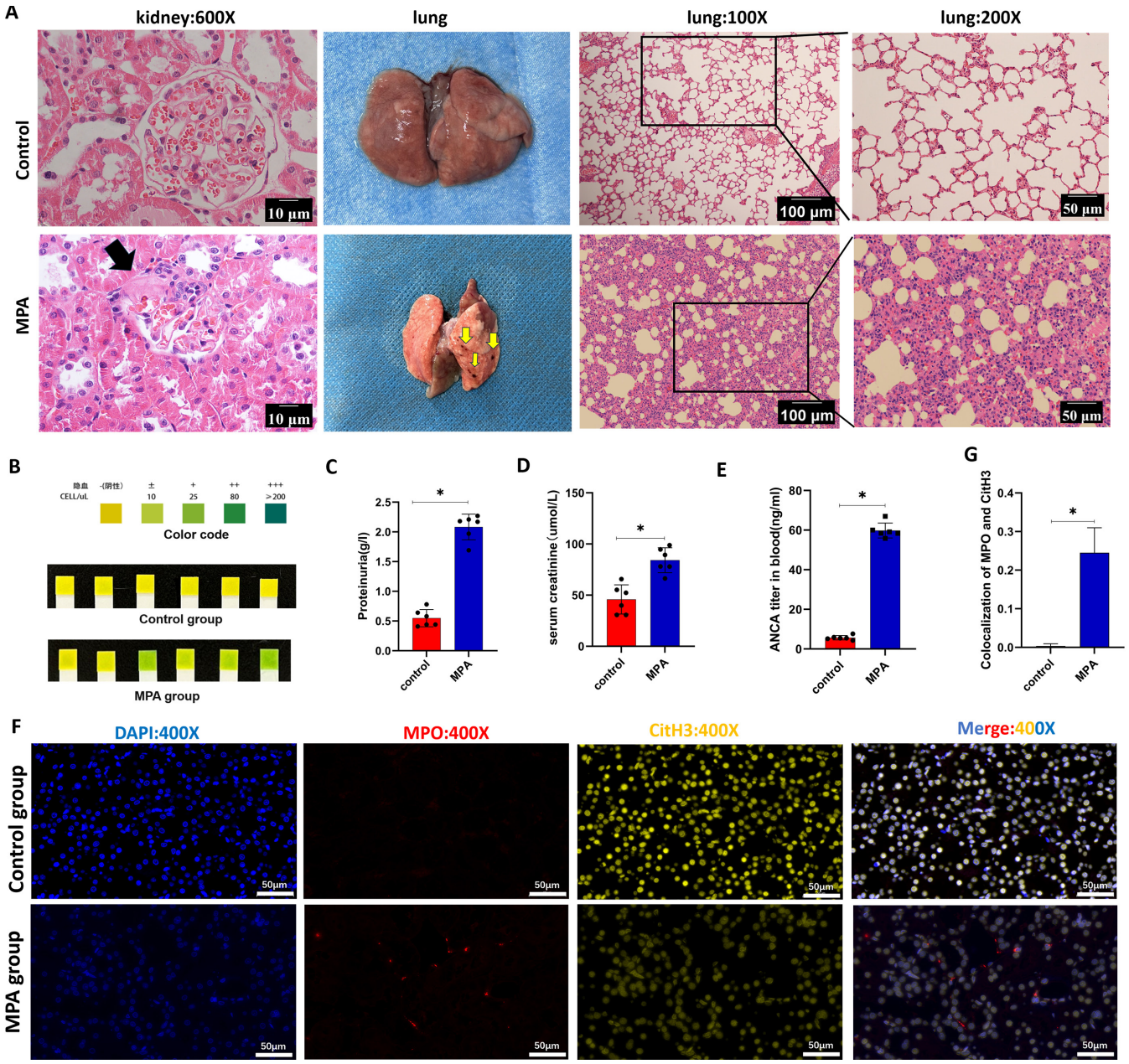

Fig. 2. Pathological characteristics in the MPA rat model.
A: Representative HE is staining images of renal and pulmonary tissues in the control and MPA groups. Cellulose exudation and infiltration of inflammatory cells are indicated by black arrows, and the presence of haemorrhagic spots in the lungs is indicated by yellow arrows, n=6.
B-**E**: Results of haematuria, proteinuria, serum creatinine, and ANCA titre tests in control and MPA rats, n=6.
F-**G**: Representative images and immune fluorescent detection results of NETs in the kidneys of control and MPA rats (DNA: blue, MPO: red; CitH3: yellow), n=6.

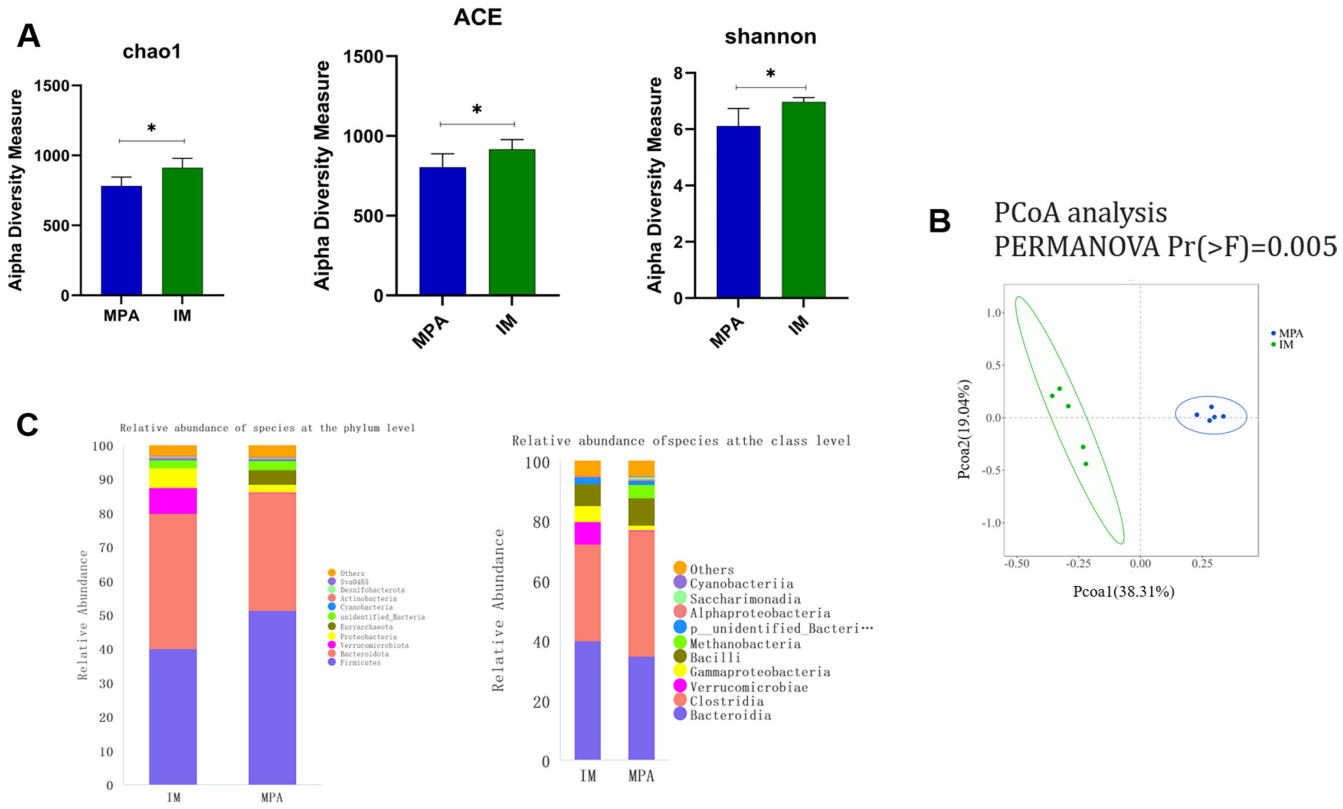

Fig. 3. Differences in gut microbiota between MPA and IM rats.
A: Boxplots showcasing alpha diversity indices (Chao1 index, ACE index, Shannon index) in faecal samples.
B: Principal coordinates analysis (PCoA) according to the Bray-Curtis beta-diversity metric.
C:The relative abundance of species at the phylum and class level.

with the TLR7 agonist imiquimod (R837) at a concentration of 0.5 mg/mL and dose of 0.1 mL per day starting on day 30 (18). In the IM+M5049 group, rats were oral gavage with the TLR7 inhibitor enpatoran (M5049) of 2.0 mg/kg per day starting from day 30 (19). The control group received sterile water by oral gavage and physiological saline by intraperitoneal injection. On the 46th day, the rats were euthanised, and various biological samples, including peripheral blood, urine, kidneys, lungs, spleen, and colon tissues, were collected for the next experimental stage.

Haematoxylin and eosin (HE) staining and immunofluorescence

Kidneys and lungs were removed and placed in fresh 4% neutral buffered paraformaldehyde for 24 h at 20–26°C, followed by paraffin embedding and histological analysis. For immunofluorescence staining, sections were probed with antibodies against TLR7 (Thermo Fisher Scientific, Waltham, MA, USA), CitH3 (Servicebio, Wuhan, China) and MPO (Servicebio, Wuhan, China), and then stained with FITC, Alexa Fluor 488- and CY3- conjugated secondary antibodies (Invitrogen, Carlsbad, CA, USA; Servicebio, Wuhan, China). Subsequently, the Image > Colour > Split Channels function and the Colocalisation Finder plugin in ImageJ software were used in order to perform quantitative analysis on different samples (ImageJ 1.53q, National Institutes of Health, USA).

Western blotting

Rat colons were removed, washed thoroughly with pre-chilled physiological saline, and the moisture on tissue surfaces was absorbed with filter paper. Colon tissues were homogenised in RIPA lysis buffer (Suolaibao, Shanghai, China). Protein concentrations were measured using a BCA Protein Assay Kit. Proteins were subjected to Western blotting with the indicated primary antibodies using established techniques.

ELISA assay

ANCA titre, interleukin-1β (IL-1β), interleukin-6 (IL-6), C-reactive protein (CRP), and tumour necrosis factor (TNF-α) were quantified with enzyme-linked immunosorbent assay (ELISA) kits (Shanghai Enzyme-linked Biotechnology Co., Ltd). In brief, abdominal aorta blood was sampled, the blood was centrifuged at 3000 x g for 15 min at 4°C, and the supernatant was collected to detect inflammatory cytokines using ELISA kit instructions.

Statistical analysis

Statistical analyses were performed using the GraphPad Prism 9.0 software (GraphPad Software, Inc.). Data are expressed as the mean ± standard deviation. Each experiment was repeated three times unless otherwise indicated. Statistical differences were determined using Student's t-test, Multiple group comparisons were analysed by one-way ANOVA and Tukey's *post-hoc* test was used to adjust the *p*-value. *p*-value <0.05 was considered statistically significant.

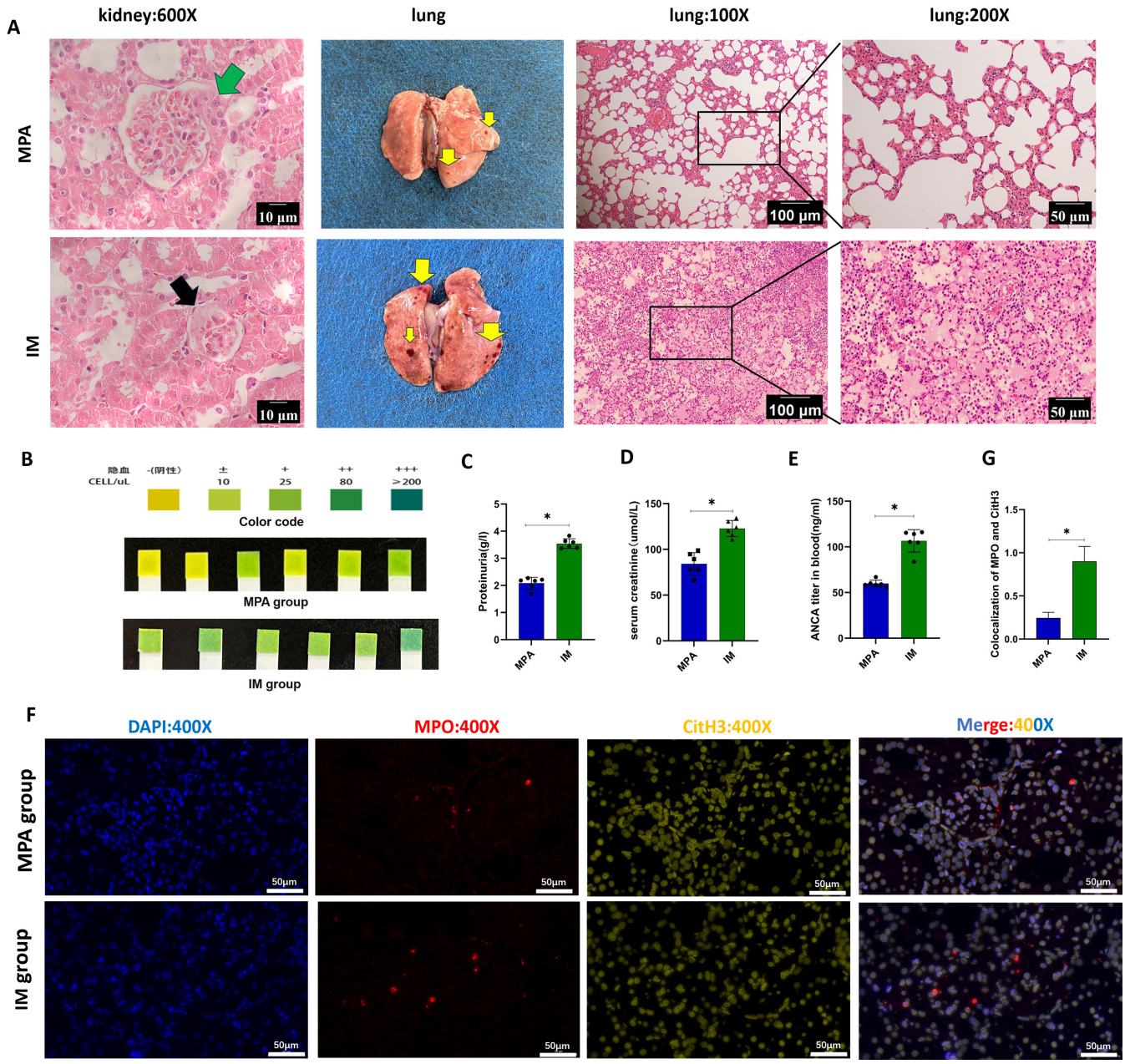

Fig. 4. Gut microbiota dysbiosis exacerbates kidney and lung injury in MPA rats.
A: Representative images of HE is staining of renal and pulmonary tissues in MPA and IM rats (gut microbiota dysbiosis rats); green arrows represent cellulose exudation, black arrows represent cellular crescents within glomeruli, yellow arrows represent pulmonary bleeding spots, n=6.
B-**E**: Results for haematuria, proteinuria, and serum creatinine in MPA and IM rats, n=6.
F-**G**: Representative images and immune fluorescent detection results of NETs in the kidneys of MPA and IM rats (DNA: blue; MPO: red; CiyH3: yellow), n=6.

Results

Pathological characteristics in the MPA rat model

On day 30 of model development, we assessed the MPA rat model. The control group exhibited kidney tissue with thin, clear glomerular capillary loops and normal endothelial/mesangial cell counts. Surrounding renal tubules appeared intact, lacking inflammatory infiltration. In contrast, the MPA group displayed glomerular inflammatory infiltration, focal segmental proliferation, fibrinous exudation, and occasional cellular crescent formation. Lung tissue in controls showed numerous polyhedral alveoli with thin walls and delicate septa, alongside normal respiratory bronchioles and vessels. Conversely, MPA-treated rats exhibited thickened alveolar septa and occasional red blood cell exudate in alveoli (Fig. 2A). MPA rats also demonstrated significant elevations in haematuria, proteinuria, serum creatinine, and ANCA titres *versus* controls (Fig. 2B-E). Immunofluorescence analysis of NET formation (MPO-red, CitH3-yellow, DAPI-blue) revealed negligible NETs in control kidneys but prominent formation in MPA kidneys (Fig. 2F-G).

Ceftriaxone sodium induced changes in the gut microbiota of MPA rats

To assess the effect of gut microbiota

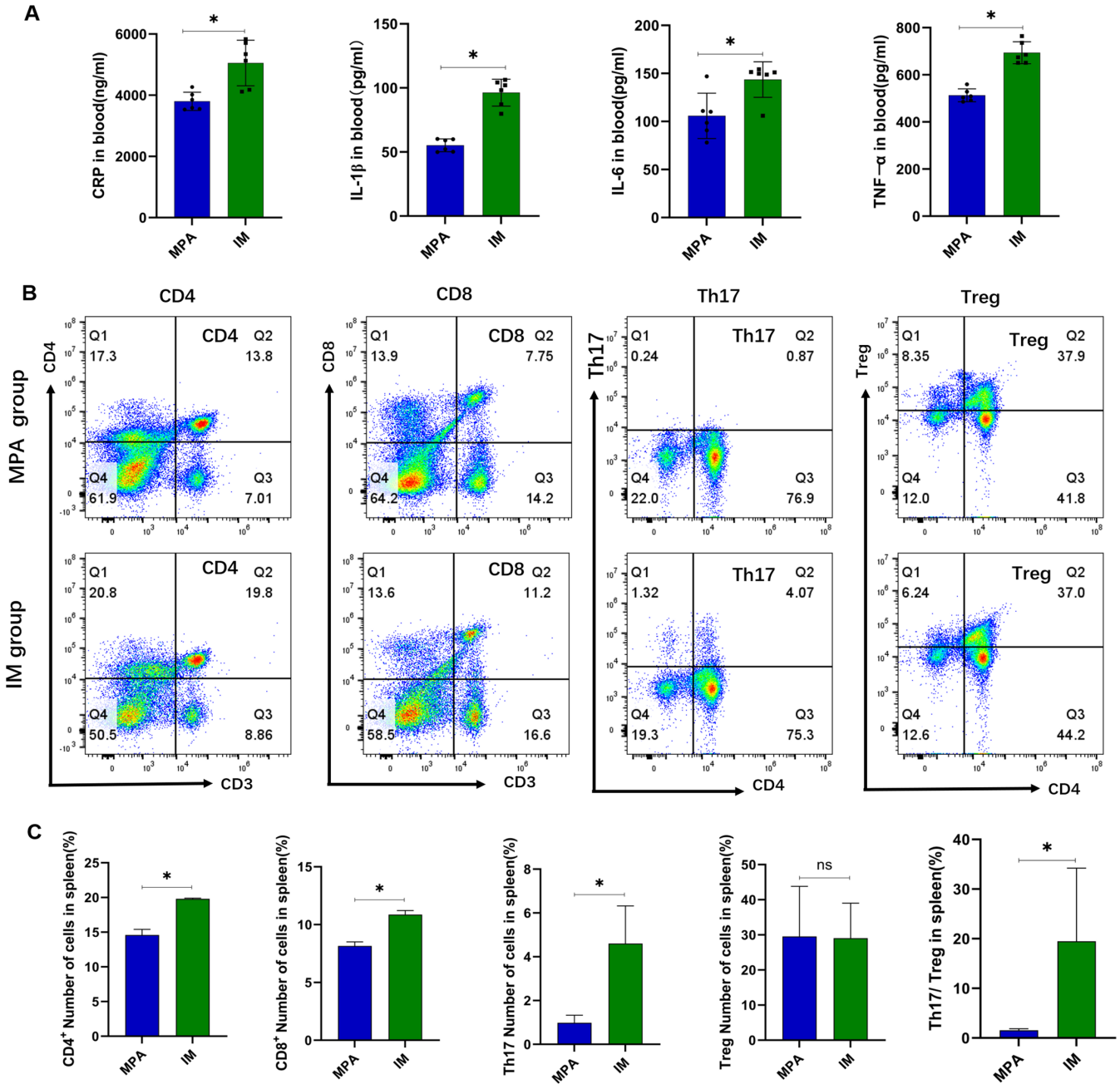

Fig. 5. Gut microbiota dysbiosis exacerbates microinflammation and disrupts immune balance in MPA rats.
A: Quantitative detection results of CRP, IL-1β, IL-6, and TNF-α in the peripheral blood of rats in the MPA and IM groups.
B: Representative images of $CD4^+$T cells ($CD3^+$ $CD4^+$ T cells), $CD8^+$T cells ($CD3^+$ $CD8^+$ T cells), Th17 cells ($CD3^+$ $CD4^+IL17A^+$ T cells), and Treg cells ($CD3^+CD4^+$ $Foxp3^+$T cells) in the spleens of the MPA and IM groups detected using flow cytometry.
C: Comparison of quantitative flow cytometry results.

dysbiosis on MPA rats, we induced gut flora dysbiosis using ceftriaxone and assessed changes in faecal microbes using 16sRNA. The results are shown in Figure 3. Alpha diversity was estimated based on the Chao1, ACE, Shannon, and observed-species indices, and indicated different abundances and taxon distributions in the MPA and IM groups, with a significant decrease in α diversity in the IM group ($p<0.05$). Similarly, β-diversity analyses based on Bray-Curtis metrics and hierarchical clustering showed significant sample separation between MPA and IM rats.

The performed relative abundance analyses at the phylum level showed that the rats in the IM group had a decreased abundance of *Firmicutes* and *Euryarchaeota;* and an increased abundance of *Bacteroidota*, *Verrucomicrobiota*, *Proteobacteria*, and *Actinobacteria*. At the class level, the microbial community showed a similar trend: the IM group had elevated levels of *Bacteroidia*, *Verrucomicrobiae,* and *Gammaproteobacteria*, whereas the abundance of *Clostridia* and *Methanobacteria* was reduced.

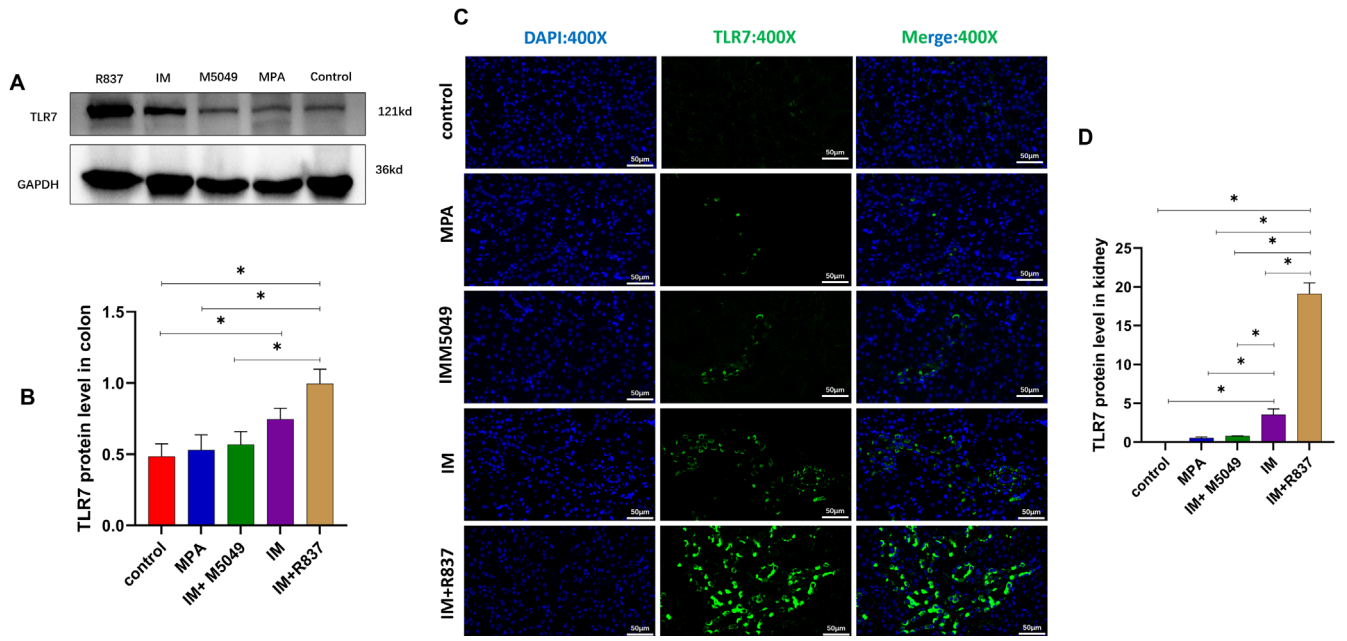

Fig. 6. Gut microbiota dysbiosis induces upregulation of TLR7 expression in MPA rats.
A-**B**: Representative images and Western blot results of colonic TLR7 expression in control, MPA, IM, IM+ M5049, and IM+R837 rats.
C-**D**: Representative images and immune fluorescent detection results of TLR7 expression in rat kidney tissues in the MPA, IM, IM+ M5049, and IM+R837 groups (DNA: Blue, TLR7: Green), n=6.

Gut microbiota dysbiosis leads to more severe kidney and lung damage and increased NET release in MPA rats

To evaluate the effects of gut microbiota dysbiosis on the kidneys and lungs of MPA rats, we assessed the extent of organ lesions using HE is staining. As shown in Figure 4, IM rats with ceftriaxone-induced gut microbiota dysbiosis developed more extensive inflammatory cell infiltration, focal hyperplasia, and fibrinoid exudates, and had more severe renal injury compared with MPA rats. In MPA rats, lungs display circular haemorrhagic spots of varying sizes, all in a bright red colour. HE staining indicated inflammatory lesions, thickened alveolar septa, and occasional red blood cell exudation into alveolar cavities. Compared with MPA rats, lung lesions were more severe in IM rats. HE staining showed loss of normal lung structure in IM rats, with marked thickening of alveolar walls and septa and extensive infiltration of neutrophils and lymphocytes. In addition, capillary damage was more pronounced, and many erythrocytes and eosinophils infiltrated into the alveolar lumen (Fig. 4A). Furthermore, IM rats exhibited more pronounced haematuria than MPA rats, with significantly higher levels of urinary protein, serum creatinine, and ANCA titres (Fig. 4B-E). Immunofluorescence analysis of kidney NET formation showed that NET formation was significantly greater in the kidneys of IM rats than in those of MPA rats (Fig. 4F-G).

Gut microbiota dysbiosis exacerbates microinflammation and disrupts immune balance in MPA rats

To further assess the effects of gut microbiota dysbiosis on MPA rats, we used ELISA kits to measure the levels of inflammatory markers such as CRP, IL-1β, IL-6, and TNF-α in the peripheral blood of MPA and IM rats. The results showed that IM rats had significantly higher levels of CRP, IL-1β, IL-6, and TNF-α than MPA rats (Fig. 5A). Flow cytometry was employed to determine the proportions of T-lymphocyte subgroups in the spleens of both rat groups. The results indicated that IM rats had a significantly higher proportion of $CD4^+$ T cells, $CD8^+$ T cells, and Th17 cells, along with an elevated Th17/Treg ratio; however, the difference in Treg cell proportion was not statistically significant (Fig. 5B-C).

Gut microbiota dysbiosis increases TLR7 expression in the colons and kidneys of MPA rats

To elucidate the specific mechanisms by which gut microbiota dysbiosis regulates the progression of MPA, we employed Western blotting to quantify TLR7 protein expression in rat colon tissues, while immunofluorescence was utilised to assess TLR7 localisation in kidneys. The results demonstrated that TLR7 protein expression was significantly higher in IM rats than in MPA rats (Fig. 6A-B). To elucidate the specific mechanisms by which gut microbiota dysbiosis regulates the progression of MPA, we employed Western blotting to quantify TLR7 protein expression in rat colon tissues, while immunofluorescence was utilised to assess TLR7 localisation in kidneys. The results demonstrated that TLR7 protein expression was significantly higher in IM rats than in E8.1 MPA rats (Fig. 6A-B). Additionally, intraperitoneal administration of R837 (a selective TLR7 agonist) in IM rats (IM+R837 group) further augmented TLR7 expression, whereas treatment with enpatoran (M5049, a specific TLR7 inhibitor) (IM+M5049 group) attenuated it. These findings confirm that R837 and

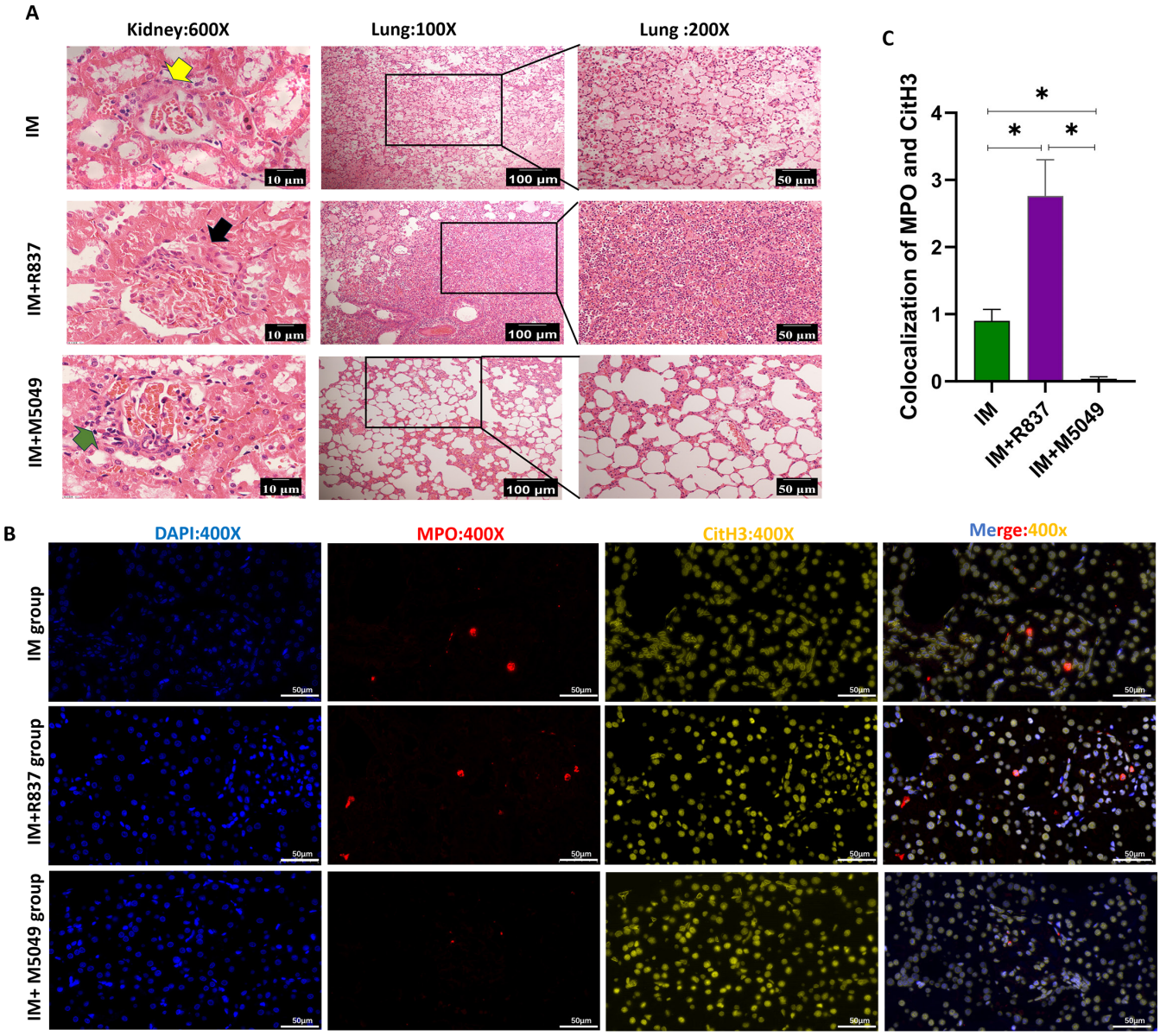

Fig. 7. Gut microbiota dysbiosis aggravates renal and pulmonary injury in MPA rats and increases the formation of kidney NETs through TLR7 regulation. **A**: Representative HE is staining images of renal and pulmonary tissues in IM, IM+R837, and IM+ M5049 rats. Fibrous exudate is indicated by yellow arrows, crescent formation is indicated by black arrows, and lymphocyte infiltration is indicated by green arrows, n=6.
B-**C**: Representative images and results of fluorescent immune detection of NETs in the kidneys of IM, IM+R837, and IM+ M5049 rats (DNA: Blue, MPO: red, yellow: CitH3), n=6.

M5049 act as agonists and inhibitors, respectively, of the TLR7 signalling pathway. Parallel immunofluorescence analysis of renal TLR7 expression mirrored these trends (Fig. 6C-D).

Gut microbiota dysbiosis aggravates kidney and lung injury and induces kidney NET release in MPA rats via TLR7

To investigate whether the exacerbation of kidney and lung damage and increase in kidney NET release in MPA rats caused by gut microbiota dysbiosis is associated with TLR7, intraperitoneal injections of R837 and M5049 were administered, followed by HE staining to observe pathological changes in kidneys and lungs. TLR7 inhibitor-injected rats (IM+ M5049 group) with attenuated kidney and lung injury. Conversely, in rats injected with the TLR7 agonist (IM+R837 group), kidney and lung damage progressed (Fig. 7A). Immunofluorescence analysis revealed that, compared to the IM group, NET formation in the kidneys was significantly higher in the IM+R837 group and substantially lower in the IM+ M5049 group (Fig. 7B-C).

Gut microbiota dysbiosis aggravates microinflammation and immune imbalance in MPA rats via TLR7

To understand whether gut microbiota dysbiosis exacerbates microinflammation and immune imbalance in MPA rats via TLR7 receptor proteins, we assessed the levels of peripheral blood inflammatory markers, including CRP, IL-1β, IL-6, and TNF-α, in rats from the IM, IM+R837, and IM+ M5049

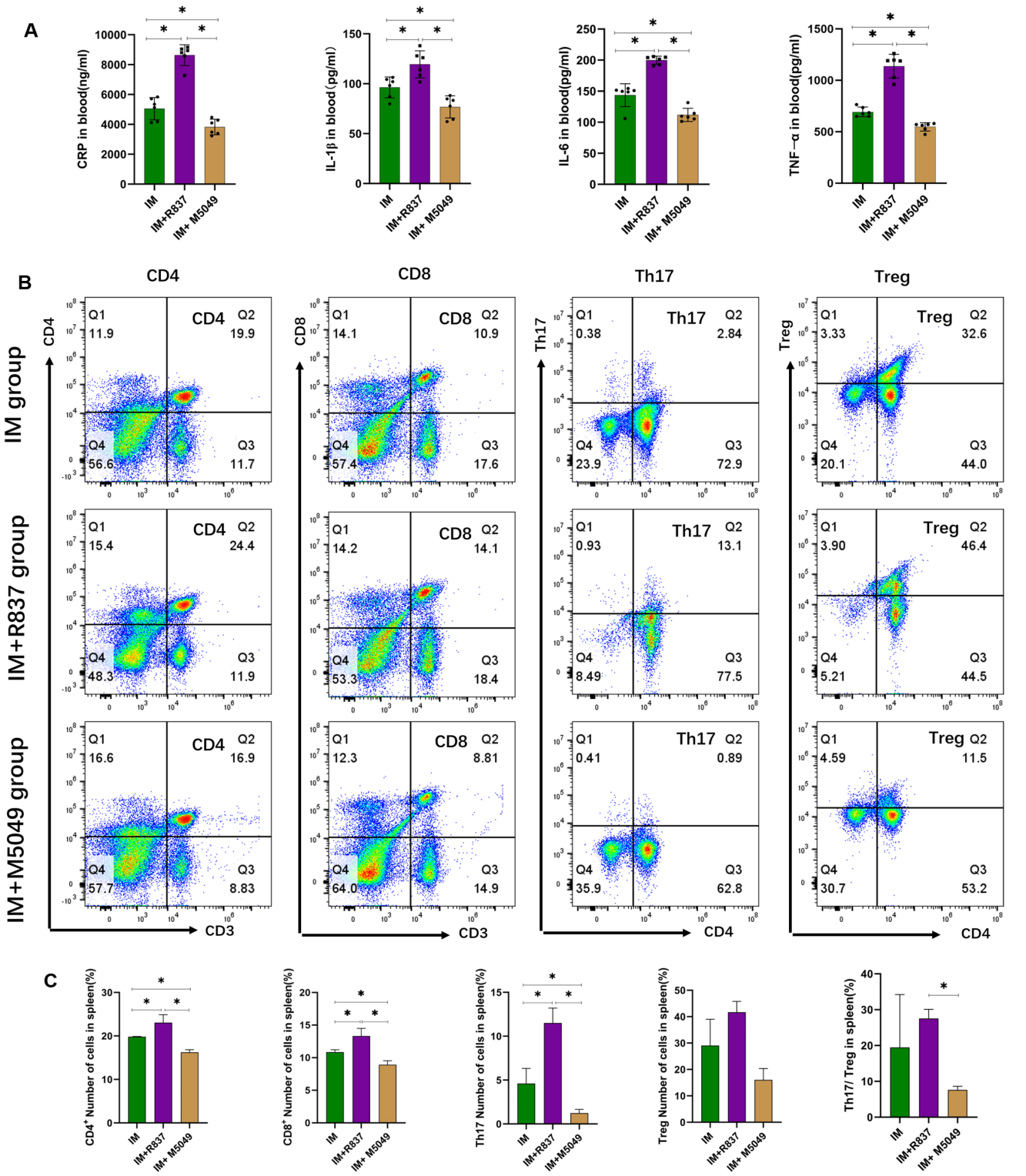

Fig. 8. Gut dysbiosis exacerbates systemic microinflammation and immune imbalance in MPA rats through TLR7 activation.
A: Comparison of quantitative detection results of CRP, IL-1β, IL-6, and TNF-α in the peripheral blood of rats in the IM, IM+R837, and IM+ M5049 groups.
B: Representative images of $CD4^+$T cells ($CD3^+$ $CD4^+$ T cells), $CD8^+$T cells ($CD3^+$ $CD8^+$ T cells), Th17 cells ($CD3^+CD4^+IL17A^+$ T cells), and Treg cells ($CD3^+CD4^+$ $Foxp3^+$T cells) in the spleens of IM, IM+R837, and IM+ M5049 rats were detected using flow cytometry.
C: Comparison of quantitative flow cytometry results.

groups using ELISA kits. Compared with the IM group, the IM+R837 group showed significantly higher levels of CRP, IL-1β, IL-6, and TNF-α. Meanwhile, the IM+ M5049 group exhibited significantly lower levels of these inflammatory markers compared to the IM group (Fig. 8A).

We then employed flow cytometry to examine the proportions of T-lymphocyte subgroups in the spleens of these three groups. Compared to the IM group, the

IM+R837 group showed a significant increase in the proportions of $CD4^+$ T, $CD8^+$ T, and Th17 cells, alongside a higher Th17/Treg ratio. Conversely, the IM+ M5049 group showed the opposite pattern, although there was no statistically significant difference in the proportion of Treg cells between the two groups (Fig. 8B-C).

Elevated TLR7 expression in kidneys of MPA patients

In order to verify the expression of TLR7 in the renal tissues of the patients with MPA, we obtained three pathological sections of renal tissues from the patients with MPA and three pathological sections of adjacent normal renal tissues from patients with cancer, all of which were sourced from The Second Affiliated Hospital of Guangxi Medical University. The immunofluorescence results showed that the expression of TLR7 in the renal tissues of MPA patients was significantly higher than that in the control group ($p<0.05$).

Discussion

The exact aetiology of MPA is currently unknown, but previous studies have indicated that NET formation is crucial (20, 21). An overabundance of NETs induces vascular damage (24), and NETs are involved in ANCA production, mediating excessive neutrophil activation, which subsequently releases inflammatory cytokines, reactive oxygen species, and lytic enzymes (22-24). NETs exacerbate kidney injury by promoting cellular crescents formation (25). Additionally, changes in lymphocyte subgroups have been associated with MPA progression. For example, an increase in $CD8^+$ T-cells in the kidneys drives disease progression in patients with MPA (26, 27). Similarly, the ratio of $CD4^+$ T cells to Th17/Treg cells is intricately linked to the immunological mechanisms underlying MPA onset and prognosis (28, 29).

In this study, an MPA rat model was successfully established using PMA/PTU, with its histopathological features and immunological changes resembling those found in human AAV (30, 31). Ceftriaxone sodium, one of the most common agents used to induce gut microbiota dysbiosis in animal models (32-34), was used in the present study to induce dysbiosis in the MPA rats. The results of the faecal 16sRNA analysis showed a significant decrease in α- and β-diversity indices, an increase in thick-walled bacterial phyla and *Streptococcus intestinalis*, and a decrease in probiotics in the ceftriaxone sodium-induced intestinal dysbiosis group of rats, which is in agreement with previous studies (32, 35, 36).

In this model, gut microbiota dysbiosis aggravates kidney and lung injury, increases NET formation in the kidneys, intensifies microinflammation, and promotes immune imbalance. Our findings suggest that gut microbiota dysbiosis can increase NET formation in the kidneys of MPA rats, elevate the systemic inflammatory response, increase counts of $CD4^+$ T, $CD8^+$ T, and Th17 cells, and disrupt immune homeostasis, leading to increased levels of inflammatory cytokines and reactive oxygen species, as well as enhanced lytic enzyme release and cellular crescent formation, which is consistent with previous research (37-39). Additionally, we observed that intestinal microbiota dysbiosis upregulated TLR7 expression in the colon and kidneys of MPA rats. To verify whether the effects of intestinal microbiota dysbiosis on MPA were mediated by TLR7, we administered TLR7 inhibitors and observed attenuation of these effects, thus confirming that the impact of intestinal microbiota dysbiosis on MPA was indeed TLR7-mediated. In our study, the performed immunofluorescence assays revealed elevated TLR7 expressions in the kidneys of MPA patients, which validates the aforementioned hypothesis. This may be achieved through the following mechanisms. First, activation of the TLR7 receptor exacerbates a series of pathological processes triggered by dysbiosis. Specifically, TLR7 activation induces the production of CXC chemokine ligand 16 (CXCL16), which in turn regulates neutrophil activation and migration and also promotes the formation of neutrophil extracellular traps (NETs) (37). Second, the binding of TLR7 to its ligand triggers the activation of quiescent autoimmune B cells, thereby facilitating autoantibody production (40-42). Third, TLR7 activation promotes the differentiation of $CD4^+$ T lymphocytes into Th17 cells through the secretion of cytokines such as interleukin-21(IL-21). (38), Increased Th17 cell populations exacerbate renal inflammation and tissue damage (25, 43), while an elevated Th17/Treg ratio impairs the anti-inflammatory effects and aggravates ANCA-associated vasculitis (AAV)-related vascular endothelial injury (44, 45). Furthermore, TLR7 activation in renal tubular epithelial cells induces increased expression of chemokines, such as Ccl2, Cxcl1, and miR-21, thereby promoting renal fibrosis and inflammation (39). Additionally, intestinal dysbiosis may activate the TLR7-MyD88-NF-κB signalling pathway, thus leading to increased levels of downstream inflammatory factors such as IL-1β, IL-6, and TNF-α, which further amplify inflammatory responses (46, 47). Finally, TLR7 activation can increase CD31 expression at the intercellular junctions between endothelial cells and leukocytes (including monocytes and macrophages), resulting in increased monocyte-macrophage infiltration into the kidneys (48). Collectively, gut microbiota dysbiosis can activate the aforementioned effects through TLR7, which collectively exacerbate kidney and lung damage and accelerate the progression of MPA. In our study, the inhibition or activation of TLR7 did not affect the number of Treg cells, a finding that contrasts with that of an earlier study (43). This could be attributed to the fact that TLR7 influences Tregs primarily by inhibiting their function rather than by reducing their number.

To our knowledge, this is the first study to investigate the role and specific mechanisms of gut microbiota dysbiosis in MPA. However, because our study involved antibiotic intervention in a rat model of MPA, we could not conclusively establish a causal relationship between gut microbiota dysbiosis and MPA levels. Further experiments at the cellular level are required to investigate the underlying mechanisms thoroughly.

References

1. HERRERA-DARIAS S, GUILLEN-CHIRINOS G, GOMEZ-CERQUERA JM: ANCA-associated vasculitis. *Med Clin* 2023; 160(10): 467. https://doi.org/10.1016/j.medcli.2022.12.006
2. NAKAZAWA D, MASUDA S, TOMARU U, ISHIZU A: Pathogenesis and therapeutic interventions for ANCA-associated vasculitis. *Nat Rev Rheumatol* 2019; 15(2): 91-101. https://doi.org/10.1038/s41584-018-0145-y
3. TANG Z, YU S, PAN Y: The gut microbiome tango in the progression of chronic kidney disease and potential therapeutic strategies. *J Transl Med* 2023; 21(1): 689. https://doi.org/10.1186/s12967-023-04455-2
4. KITCHING AR, ANDERS HJ, BASU N *et al*.: ANCA-associated vasculitis. *Nat Rev Dis Primers* 2020; 6(1): 71. https://doi.org/10.1038/s41572-020-0204-y
5. NASSER M, COTTIN V: The respiratory system in autoimmune vascular diseases. *Respiration* 2018; 96(1): 12-28. https://doi.org/10.1159/000486899
6. LI ZY, MA TT, CHEN M, ZHAO MH: The prevalence and management of anti-neutrophil cytoplasmic antibody-associated vasculitis in China. *Kidney Dis* (Basel) 2016; 1(4): 216-23. https://doi.org/10.1159/000441912
7. DELVINO P, BALDINI C, BONACINI M *et al*.: Systemic vasculitis: one year in review 2025. *Clin Exp Rheumatol* 2025; 43(4): 553-62. https://doi.org/10.55563/clinexprheumatol/oyqz1p
8. LAN J, ZHU Y, RAO J *et al*.: MTOR gene polymorphism may be associated with microscopic polyangiitis susceptibility in a Guangxi population of China. *Gene* 2023; 854: 147101. https://doi.org/10.1016/j.gene.2022.147101
9. CHEN M, YU F, ZHANG Y, ZHAO MH: Clinical [corrected] and pathological characteristics of Chinese patients with antineutrophil cytoplasmic autoantibody associated systemic vasculitides: a study of 426 patients from a single centre. *Postgrad Med J* 2005; 81(961): 723-27. https://doi.org/10.1136/pgmj.2005.034215
10. WATTS RA, SCOTT DGI, JAYNE DRW*et al*.: Renal vasculitis in Japan and the UK are there differences in epidemiology and clinical phenotype? *Nephrol Dial Transplant* 2008; 23(12): 3928-31. https://doi.org/10.1093/ndt/gfn354
11. AIYEGBUSI O, FRLETA-GILCHRIST M, TRAYNOR JP *et al*.: ANCA-associated renal vasculitis is associated with rurality but not seasonality or deprivation in a complete national cohort study. *RMD Open* 2021; 7(2): e001555. https://doi.org/10.1136/rmdopen-2020-001555
12. HUNTER RW, WELSH N, FARRAH TE, GALLACHER PJ, DHAUN N: ANCA associated vasculitis. *BMJ* 2020; 369: m1070. https://doi.org/10.1136/bmj.m1070
13. TRECCANI M, VESCHETTI L, PATUZZO C, MALERBA G, VAGLIO A, MARTORANA D: Genetic and non-genetic contributions to eosinophilic granulomatosis with polyangiitis: current knowledge and future perspectives. *Curr Issues Mol Biol* 2024; 46(7): 7516-29. https://doi.org/10.3390/cimb46070446
14. KRONBICHLER A, LEE KH, DENICOLO S *et al*.: Immunopathogenesis of ANCA-associated vasculitis. *Int J Mol Sci* 2020; 21(19): 7319. https://doi.org/10.3390/ijms21197319
15. OOI JD, JIANG JH, EGGENHUIZEN PJ *et al*.: A plasmid-encoded peptide from Staphylococcus aureus induces anti-myeloperoxidase nephritogenic autoimmunity. *Nat Commun* 2019; 10(1): 3392. https://doi.org/10.1038/s41467-019-11255-0
16. NICCOLAI E, BETTIOL A, BALDI S *et al*.: Gut microbiota and associated mucosal immune response in eosinophilic granulomatosis with polyangiitis (EGPA). *Biomedicines* 2022; 10(6): 1227. https://doi.org/10.3390/biomedicines10061227
17. ZHAO Z, WANG B, MU L *et al*.: Long-term exposure to ceftriaxone sodium induces alteration of gut microbiota accompanied by abnormal behaviors in mice. *Front Cell Infect Microbiol* 2020; 10:258. https://doi.org/10.3389/fcimb.2020.00258
18. VAN DER FITS L, MOURITS S, VOERMAN JSA *et al*.: Imiquimod-induced psoriasis-like skin inflammation in mice is mediated via the IL-23/IL-17 axis. *J Immunol* 2009; 182(9): 5836-45. https://doi.org/10.4049/jimmunol.0802999
19. VLACH J, BENDER AT, PRZETAK M *et al*.: Discovery of M5049: a novel selective toll-like receptor 7/8 inhibitor for treatment of autoimmunity. *J Pharmacol Exp Ther* 2021; 376(3): 397-409. https://doi.org/10.1124/jpet.120.000275
20. SUN XJ, LI ZY, CHEN M: Patho genesis of anti-neutrophil cytoplasmic antibody-associated vasculitis. *Rheumatol Immunol Res* 2023; 4(1):11-21. https://doi.org/10.2478/rir-2023-0003
21. TSUKUI D, KIMURA Y, KONO H: Pathogenesis and pathology of anti-neutrophil cytoplasmic antibody (ANCA)-associated vasculitis. *J Transl Autoimmun* 2021; 4: 100094. https://doi.org/10.1016/j.jtauto.2021.100094
22. SHIRATORI-ASO S, NAKAZAWA D: The involvement of NETs in ANCA-associated vasculitis. *Front Immunol* 2023; 14: 1261151. https://doi.org/10.3389/fimmu.2023.1261151
23. LEE KH, KRONBICHLER A, PARK DDY *et al*.: Neutrophil extracellular traps (NETs) in autoimmune diseases: a comprehensive review. *Autoimmun Rev* 2017; 16(11): 1160-73. https://doi.org/10.1016/j.autrev.2017.09.012
24. SU B, MAO X, YIN B *et al*.: TIM-3 regulates the NETs-mediated dendritic cell activation in myeloperoxidase-ANCA-associated vasculitis. *Clin Exp Rheumatol* 2021; 39 (Suppl. 129): S13-20. https://doi.org/10.55563/clinexprheumatol/6y0bjb
25. NAKAZAWA D, MARSCHNER JA, PLATEN L, ANDERS HJ: Extracellular traps in kidney disease. *Kidney Int* 2018; 94(6): 1087-98. https://doi.org/10.1016/j.kint.2018.08.035
26. LINKE A, TIEGS G, NEUMANN K: Pathogenic T-cell responses in immune-mediated glomerulonephritis. *Cells-Basel* 2022; 11(10): 1625. https://doi.org/10.3390/cells11101625
27. MUELLER A, ZHAO Y, CICEK H *et al*.: Transcriptional and clonal characterization of cytotoxic t cells in crescentic glomerulonephritis. *J Am Soc Nephrol* 2023; 34(6): 1003-18. https://doi.org/10.1681/asn.0000000000000116
28. LIAO Z, TANG J, LUO L *et al*.: Altered Gcirculating CCR6 and CXCR3 T cell subsets are associated with poor renal prognosis in MPO-ANCA-associated vasculitis. *Arthritis Res Ther* 2021; 23(1): 194. https://doi.org/10.1186/s13075-021-02576-x
29. CLOTTU AS, HUMBEL M, FLUDER N, KARAMPETSOU MP, COMTE D: Innate lymphoid cells in autoimmune diseases. *Front Immunol* 2021; 12: 789788. https://doi.org/10.3389/fimmu.2021.78978 8
30. BINDA V, MORONI G, MESSA P: ANCA-associated vasculitis with renal involvement. *J Nephrol* 2018; 31(2): N197-208. https://doi.org/10.1007/s40620-017-0412-z
31. SACOTO G, BOUKHLAL S, SPECKS U, FLORES-SUAREZ LF, CORNEC D: Lung involvement in ANCA-associated vasculitis. *Presse Med* 2020; 49(3): 104039. https://doi.org/10.1016/j.lpm.2020.104039
32. ZENG Z, YUE W, KINED C *et al*.: Bacillus licheniformis reverses the environmental ceftriaxone sodium-induced gut microbial dysbiosis and intestinal inflammation in mice. *Ecotoxicol Environ Saf* 2023; 257: 114890. https://doi.org/10.1016/j.ecoenv.2023.114890
33. AVAGLIANO C, CORETTI L, LAMA A *et al*.: Dual-hit model of parkinson's disease: impact of dysbiosis on 6-hydroxydopamine-insulted mice-neuroprotective and anti-inflammatory effects of butyrate. *Int J Mol Sci* 2022; 23(12): 6367. https://doi.org/10.3390/ijms23126367
34. LUO X, XU B, XIONG T *et al*.: Hepatic dysfunction induced by intestinal dysbacteriosis mainly manifests as immunologic abnormity in mice. *Pathog Dis* 2020; 78(6): ftaa041. https://doi.org/10.1093/femspd/ftaa041
35. DUCLOT F, WU L, WILKINSON CS, KABBAJ M, KNACKSTEDT LA: Ceftriaxone alters the gut microbiome composition and reduces alcohol intake in male and female Sprague-Dawley rats. *Alcohol* 2024; 120: 169-78. https://doi.org/10.1016/j.alcohol.2024.01.006
36. APARECIDA DOS REIS LOUZANO S, DE MOURA M, LOPES DA CONCEICAO L, ANTONIO DE OLIVEIRA MENDES T, GOUVEIA PELUZIO MC: Ceftriaxone causes dysbiosis and changes intestinal structure in adjuvant obesity treatment. *Pharmacol Rep* 2022; 74(1): 111-23. https://doi.org/10.1007/s43440-021-00336-x
37. LU J, ZHONG X, GUO C *et al*.: TLR7-MyD88-DC-CXCL16 axis results neutrophil activation to elicit inflammatory response in pustular psoriasis. *Cell Death Dis* 2023; 14(5): 315. https://doi.org/10.1038/s41419-023-05815-y
38. TANG J, CHENG, YI X *et al*.: Factor L2 ameliorates the progression of K/BxN serum-induced arthritis by blocking TLR7 mediated IRAK4/IKKβ/IRF5 and NF-kB signaling pathways. *Front Pharmacol* 2021; 12: 773592. https://doi.org/10.3389/fphar.2021.773592
39. KIM J, HA S, SON M *et al*.: TLR7 activation by miR-21 promotes renal fibrosis by activating the pro-inflammatory signaling pathway in tubule epithelial cells. *Cell Commun Signal* 2023; 21(1): 215. https://doi.org/10.1186/s12964-023-01234-w
40. BROWN JG, CANETE PF, WANG H *et al*.:

TLR7 gain-of-function genetic variation causes human lupus. *Nature* 2022; 605(7909): 349-56. https://doi.org/10.1038/s41586-022-04642-z

41. SUTHERS AN, SARANTOPOULOS S: TLR7/TLR9- and B Cell receptor-signaling crosstalk: promotion of potentially dangerous B Cells. *Front Immunol* 2017; 8: 775. https://doi.org/10.3389/fimmu.2017.00775
42. MAURO D, MANOU-STATHOPOULOU S, RIVELLESE F *et al*.: UBE2L3 regulates TLR7-induced B cell autoreactivity in systemic lupus erythematosus. *J Autoimmun* 2023; 136: 103023. https://doi.org/10.1016/j.jaut.2023.103023
43. DOLFF S, WITZKE O, WILDE B: Th17 cells in renal inflammation and autoimmunity. *Autoimmun Rev* 2019; 18(2): 129-36. https://doi.org/10.1016/j.autrev.2018.08.006
44. ZHU X, LI S, ZHANG Q *et al*.: Correlation of increased Th17/Treg cell ratio with endoplasmic reticulum stress in chronic kidney disease. *Medicine* (Baltimore) 2018; 97(20): e10748. https://doi.org/10.1097/md.0000000000010748
45. LUO Y, GUJ O, ZHANG P *et al*.: Mesenchymal stem cell protects injured renal tubular epithelial cells by regulating mTOR-mediated Th17/Treg axis. *Front Immunol* 2021; 12: 684197. https://doi.org/10.3389/fimmu.2021.684197
46. GAO J, CHEN H, XU L *et al*.: Effects of intestinal microorganisms on influenza-infected mice with antibiotic-induced intestinal dysbiosis, through the TLR7 signaling pathway. *Front Biosci* (Landmark Ed) 2023; 28(3): 43. https://doi.org/10.31083/j.fbl2803043
47. WU S, JIANG ZY, SUN YF *et al*.: Microbiota regulates the TLR7 signaling pathway against respiratory tract influenza a virus infection. *Curr Microbiol* 2013; 67(4): 414-22. https://doi.org/10.1007/s00284-013-0380-z
48. MURAKAMI Y, FUKUI R, TANAKA R *et al*.: Anti-TLR7 antibody protects against lupus nephritis in nzbwf1 mice by targeting B cells and patrolling monocytes. *Front Immunol* 2021; 12: 777197. https://doi.org/10.3389/fimmu.2021.777197